Design of a Two-Phase Loop Thermosyphon for Telecommunications System (Ⅱ)
— Analysis and Simulation —

Won Tae Kim*, Kwang Soo Kim and Young Lee*****

(Received August 11, 1997)

A computer simulation is performed for a two-phase loop thermosyphon for the B-ISDN telecommunications. The aim of this code development is to provide capabilities to predict the affects of many variables on the performance of the proposed TLT system using different empirical correlations obtained from the literature for the evaporation and condensation, and the shape factors available. In the present study, the simulation code is based on the sectorial thermal resistance network built on the flow regimes of the two-phase flows involved. The nodal resistances are solved by the typical Gauss-Seidal iteration method. The code can predict whether the proposed design is possible based on the flooding limit calculation of the system and its results are compared with the experimental results.

Key Words: Thermosyphon, Sectorial Thermal Resistance, Simulation, Two-Phase Flow, Shape Factor

Nomenclature

A	: Area (m^2)
A_f	: Flow area occupied by liquid phase (m^2)
A_g	: Flow area occupied by vapour phase (m^2)
a	: Evaporator thickness (m)
A_x	: Cross sectional area (m^2)
b	: Evaporator width (m)
C	: Parameter
C_{pl}	: Specific heat of saturated liquid (J/kgK)
C_{sf}	: A constant on Rohsenow's pool boiling correlation
D	: Outer diameter of tube (m), parameter
d	: Iinner diameter (m)
D_h	: Hydraulic diameter (m)
F	: Frictional parameter
f	: Friction factor
G	: Mass flux (kg/m^2s)
g	: Acceleration due to gravity (m^2/s)
H	: Specific enthalpy (J/kg)
h	: Heat transfer coefficient (W/m^2 K), evaporator depth (m)
H_{fluid}	: Specific enthalpy of fluid (J/kg)
H_f	: Specific enthalpy of saturated liquid (J/kg)
H_{fg}	: Latent heat of evaporation (J/kg)
k	: Thermal conductivity (W/m K)
L	: Length (m)
Nu	: Nusselt number
ΔP_a	: Acceleration pressure drop
ΔP_f	: Frictional pressure drop
ΔP_h	: Hydraulic pressure drop
P	: Pressure (Pa)
$(dP/dy)_p$	: Pressure gradient
Pr	: Prandtl number
Q	: Heat transfer rate (W)
q	: Heat flux (W/cm^2)
R	: Resistance (K/W)
r	: Radius (m)
Ra	: Rayleigh number
Re	: Reynolds number
S	: Shape factor, defined as eqn. (2)

* Department of Industrial Engineering, Kongju National University, Chungnam, Korea
** Packaging Technology Section, Electronics and Telecommunications Research Institute(ETRI), Taejon, Korea
*** Department of Mechanical Engineering, University of Ottawa, Ottawa, Ontario, Canada

T, t : Temperature (°C)
Δt : Temperature difference between the heater and air (°C)
TCT : Two-phase closed thermosyphon
TLT : Two-phase loop thermosyphon
U_T : Overall heat transfer coefficient (W/m^2 K)
v : Liquid or vapor flow velocity
W : Mass rate of flow (kg/s)
WF : Working fluid
W_f : Mass rate of flow of liquid phase (kg/s)
W_g : Mass rate of flow of gas phase (kg/s)
We : Weber number
X : Lockhart-Martinelli parameter
x : Vapor quality
y : Axis

Subscrbpts

a : Acceleration in pressure gradient and pressure drop
air : Surrounding air
b : Bulk, boiling, bottom, bended section in Appendix E
$cold$: Cold section
c, $cond$: Condensation, condenser section
$conv$: Convection
cr : Critical
ct : Condenser tube
e : Equivalent
ev : Evaporation, evaporator
$e3$: Effective in dry-out region
ea : Average evaporator
eb : Average bulk
esb : Effective subcooling boiling
ew : Average evaporator wall
f : Fluid, f is frictional for pressure drop term
f, tp : Two-phase frictional pressure drop
do : Dry-out region
fil : Filler
g : Gas, vapor state
h : Heater, hot for Rescb, hydraulic for pressure drop
hot : Heating section
i : Inner
l : Liquid, unit length
$loop$: Thermosyphon loop
lp : Liquid-phase
max : Maximum
mis : Miscellaneous
o : Outer
pl : Evaporator plate
s, sat : Saturation
scb : Subcooled boiling
T : Total
t : Tube
tp : Two-phase
tr : Transporting section
v : Vapour
w : Wall

Greek Letters

α : Void fraction ($\alpha = A_g/A_T$)
γ : Inclination angle (degree)
δ : Thickness (m)
η : Efficiency
θ : Bended angle
μ : Viscosity (kg/ms)
ρ : Density (kg/m^3)
σ : Suface tension (N/m)
φ : Diameter
Ψ : Defined in Appendix E
ζ : Loss coefficient

1. Introduction

A purely analytical solution for the proposed TLT explained in the proceeding paper is not possible due to the two-phase fluid flow involved. The aim of the code development is to provide the capabilities to predict many variables which would affect the performance of the proposed cooling system using the TLT of the present design under the different empirical correlations for the evaporation and condensation, and the shape factors available in the literature.

The heat transfer in the single phase forced convection region was correlated early by Sieder & Tate (1936) and this correlation was used to estimate the local heat transfer coefficient. There are many correlations available to predict the conditions necessary for boiling. The correlation by Sato and Matsumura (1964) was used to

predict the minimum heat flux necessary to sustain boiling. In this region where the bubbles condense in the fluid and give up their latent heat, highly localized nucleate boiling is initially superimposed on the heat flux due to forced convection at the wall. Ali and McDonald (1977) evaluated the effective heat transfer coefficient for this region. Even though numerous correlations are available in the literature, pool boiling correlation by Rohsenow (1952) is the most widely used one in the nucleate boiling coefficient. Lavin & Young (1956) correlated the determination of the transition from two-phase forced convection to the liquid deficient region. And Rhee and Young (1974) correlated x_{cr} for dryout occurred if the quality exceeded the critical value.

Lockhart & Martinelli (1949) correlated the relationship between the two-phase and the single-phase frictional pressure drops for the vapor and liquid phases flowing separately. From their work, the parameter was empirically determined in terms of Lockhart Martinelli parameter X. The fin efficiency of circular or rectangular fins attached to the TLT involved mathematically Bessel functions, which could usually be represented in tabular and graphical forms. For analysis and simulation, approximate but reasonably accurate, empirical expressions were presented by McQuiston and Tree (Hewitt, et al., 1994)

In the present study, a new code based on the sectorial thermal resistance using finite difference/element methods is built on the flow regimes of the two-phase flows involved, because some of the heat transfer mode involved in the *loop type* is that of flow boiling. The code would also be identified for the proposed design on two-phase heat transfer limits, namely burn-out and dry-out.

2. Theoretical Background

2.1 Sectorial thermal resistance network

Under the steady-state conditions of the test, the sectorial thermal resistance model as shown in Fig. 1 is used to estimate the heat transfer rate of the present cooling system. The sectorial thermal resistance between the hot section and the cold section can be written as:

$$Q=\frac{\Delta t}{\Sigma R},\ \Sigma R=R_T=\frac{1}{U_T} \tag{1}$$

where

$$R_T=R_{hot}+R_{loop}+R_{cold}$$
$$R_{hot}=R_{fil}+R_{pl}$$
$$R_{loop}=R_{ev}+R_{tr}+R_{cond}$$
$$R_{cold}=R_{ct}+R_{conv}$$
$$R_{fil}=\frac{\delta_{fil}}{K_{fil}A_h}$$
$$R_{pl}=\frac{1}{k_{pl}S},\ \text{where } S \text{ is defined as}$$
$$S=\frac{\left[5.7+\frac{b}{2a}\right]}{\left[\ln\frac{3.5h}{b^{0.25}a^{0.75}}\right]}\ \text{by Kutateladze (1963)} \tag{2}$$
$$R_{ev}=\frac{1}{h_{ev}\pi dL_h}$$
$$R_{cond}=\frac{1}{h_c\pi dL_c}$$
$$R_{ct}=\frac{\ln(D/d)}{2\pi k_t L_c}$$
$$R_{conv}=\frac{1}{h_{conv}\eta_T A_T}$$

where the thermal resistance method requires a number of empirical correlations for various thermal resistance. Several empirical correlations

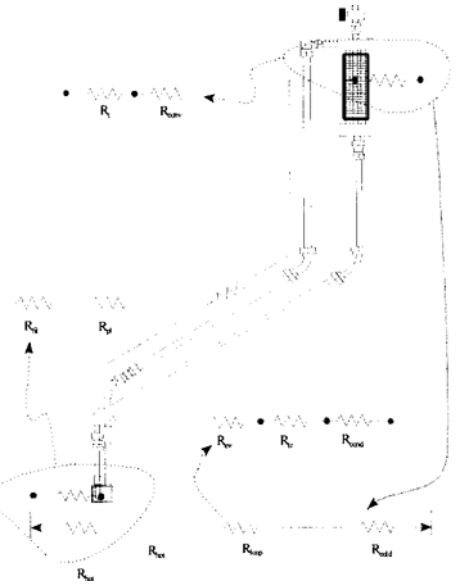

Fig. 1 Schematic of sectorial resistance network.

were proposed for flow boiling (Mathur, 1996), condensation (Mahuer, 1996), enhanced forced (Holman, 1996), and free convection (Bejan, 1993).

2.2 Analysis for programming

As seen in Fig. 1, the resistance, R_{loop}, must be determined through various flow regimes involved. In order to calculate the heat transfer, pressure drop, and the void fraction in the thermosyphon loop, it is necessary to subdivide the loop into a number of short elemental lengths, along which the local values of the pressure gradient, heat flux, etc. are to be calculated. In the simulation of a loop-type two-phase thermosyphon, virtually every and all possible modes of two-phase flow and heat transfer must be considered.

The working fluid of the loop thermosyphon enters at the bottom of the evaporator section as saturated/subcooled liquid in either laminar or turbulent flow with developing momentum and thermal boundary layers. As the fluid rises up the thermosyphon, its pressure and hence saturation temperature drop along the flow channel. As the fluid progresses along the thermosyphon, the vapor fraction and hence the velocity increases. This may result in two-phase forced convection dominant and various flow regimes may occur in the vapor header (e. g., separated, wavy, slug, bubbly, or annular flow). In the condenser, only film condensation with negligible vapor velocity is assumed. If the condenser is partially flooded, the mode of heat transfer in the flooded region becomes single-phase liquid forced convection.

From the assumption of steady state equilibrium flow, the vapor quality is defined as:

$$x=\frac{H_{fluid}-H_f}{H_{fg}}=\frac{W_g}{W_g+W_f}, \text{ and } 1-X=\frac{W_f}{W_g+W_f} \tag{3}$$

Inside the loop, the void fraction can be defined as the ratio of the flow area occupied by vapor to the total flow area

Mean density :

$$\rho_{mean}=\alpha\rho_v+(1-\alpha)\rho_l \tag{4}$$

Phase velocities:

$$V_l=\frac{W_l}{\rho_l A_x(1-\alpha)} \text{ and } v_v=\frac{W_v}{\rho_v A_x \alpha} \tag{5}$$

2.3 Conservation equation

Mass conservation

For the steady state flow the conservation of mass equation must be satisfied,

$$\frac{dW}{dy}=0 \tag{6}$$

Momentum conservation

For the steady state flow the momentum equation is

$$-\frac{dP}{dy}=\left(\frac{dP}{dy}\right)F+G^2\frac{d}{dy}\left[\frac{x^2}{\rho_g\alpha}\right]+g\sin\theta[\alpha\rho_g+(1-\alpha)\rho_f]+\left(\frac{dP}{dy}\right)_{mis} \tag{7}$$

In a closed two-phase loop thermosyphon, the summation must be zero.

Energy conservation

The amount of heat transferred to a mixture per unit length, q_1, is equal to the rate of the enthalpy change with mixture, neglecting the changes in the potential and kinetic energies.

$$q_1=\frac{d}{dy}(GH)=G\frac{dH}{dy} \tag{8}$$

The estimation of the mass flow rate for the evaporator section may be done by the following method. The heat added in the evaporator section may be estimated by:

$$W=\frac{H_{ea}A_{ev}(t_{ew}-t_{eb})}{H_{fg}x_{ev}} \tag{9}$$

With the estimation of the evaporator inlet pressure, temperature and the mass flow rate, the program proceeds to calculate the heat transfer and pressure drop for the evaporator element.

2.4 Phase flow region

2.4.1 Single-phase flow region

In this region, the working fluid enters the evaporator in a subcooled state and hence is all liquid at the entrance. Heat transfer takes place by single phase forced convection and the pressure decreases as the fluid progresses up. For the

calculation of the heat transfer in the single phase forced convection region, the correlations by Sieder & Tate (1936) were used to estimate the local heat transfer coefficient, i. e. ,

For laminar flow:

$$Nu=1.24\left[\frac{RePr}{L/D}\right]^{1/3}\left(\frac{\mu}{\mu_s}\right)^{0.14} \tag{10}$$

As the flow progresses up the evaporator, the pressure drops and hence the saturation temperature decreases. The bulk fluid temperature and the wall temperature increase along the length of the section of the evaporator. When the wall temperature exceeds the local saturation temperature by a sufficient amount (even when the bulk fluid temperature is below the saturation temperature) the first nucleation site becomes activated. If boiling takes place when the bulk fluid temperature is below the saturation temperature, it is termed subcooled nucleate boiling. The equations by Collier (1972) were used for the calculation of the pressure drop in this region.

There are many correlations available to predict the conditions necessary for boiling. These correlations are to predict the wall superheat to sustain boiling. However these may be used to predict the minimum heat flux required to maintain subcooled boiling in a flow boiling situation. The correlation of Sato and Matsumura (1964) were used to predict the minimum heat flux necessary to sustain boiling, given as:

$$(t_w-t_{sat})^2=\frac{8\sigma t_{sat}q}{H_{fg}\rho_v k_j} \tag{11}$$

Other correlations are also to be tried to find the best fit in this simulation. Without vapor bubbles, in the case of the system startup, a much greater wall superheat is required to initiate the bubble growth. In the program, to predict this phenomena, the following conditions are considered.

$x<0$: subcooling
$x>1$: superheating

Once subcooled nucleate boiling has been initiated, vapor bubbles formed at the wall detach and move into the bulk of the fluid. Since the bulk fluid temperature is less than the saturation temperature, the bubbles condense in the fluid and give up their latent heat. In this region highly localized nucleate boiling is initially superimposed on the heat flux due to forced convection at the wall. Ali and McDonald (1977) evaluated the effective heat transfer coefficient for this region from the following relation.

$$H_{esb}=[H_b^p+H_{fp}^p]^{1/p}, \text{ where } p=2-\frac{(t_{sat}-t_f)}{(t_{sat}-t_f)_{ib}} \tag{12}$$

where superscript p is unity at the point of incipient boiling. In the subcooled nucleate boiling region, the vapor quality is zero (based on the enthalpy), even though the void fraction may be sufficient to cause an increase in the velocity of the fluid. For this region, the single-phase forced convection is considered.

$$Re_{scb}=\frac{V_l D_h \rho_{mean}}{\mu_l} \tag{13}$$

In the subcooled nucleate boiling region it is assumed that the fluid is thoroughly mixed due to condensing of the vapor bubbles and hence the void fraction is calculated based on the homogenous model.

$$\alpha=\frac{1}{\left[1+\frac{(1-X_{scb})}{X_{scb}}\left(\frac{\rho_v}{\rho_l}\right)\right]} \tag{14}$$

The following quality is used to calculate the void fraction.

$$X_{scb}=\frac{q_b}{W_T h_{fg}} \tag{15}$$

where q_b is the heat transfer due to boiling. Even though the void fraction and the quality in the subcooled region are of very small magnitude, the pressure drop would be lower in comparison to that of single-phase liquid flow. The method of estimation of the pressure drop will be discussed in the pressure drop calculation for two-phase region. As the fluid progresses up the evaporator, the bulk fluid temperature would eventually be equal to the saturation temperature, when saturated nucleate boiling starts. From Rohsenow's correlation (Holman, 1996), q_b is calculated as

$$q_b=\mu_l H_{fg}\left[g\frac{(\rho_l-\rho_g)}{\sigma}\right]^{1/2}\left[\frac{c_{pl}(t_w-t_{sat})}{H_{fg}C_{SF}\mathrm{Pr}^{1.7}}\right]^s$$

(16)

where C_{SF} and s are constant for a given working fluid/heating surface combination. In the present simulation code, 0.013 (water-copper) for C_{SF} and the value of s 1.0 for water and 1.7 for other liquids are used.

2.4.2 Two-phase forced convection

At the point where the bulk fluid temperature reaches the saturation temperature, a two-phase flow heat transfer coefficient h_{tp} is estimated using correlations from the literature shown by Mathur(1996). The Lockhart & Martinelli (1972) correlations are used to relate the two -phase frictional pressure drop to the single -phase frictional pressure drops for the vapor and liquid phases following separately given as.

$$\Phi_{ij}^2=\frac{\Delta P_{tp}}{\Delta P_{lp}} \tag{17}$$

Subscript ij represents the conditions of liquid and the vapor phases respectively. The parameter N is empirically determined in terms of Lockhart Martinelli parameter X. Four such conditions exist for the mixture. Whole equations used in the calculation of two-phase pressure drop are presented in Collier (1972).

2.4.3 Transition from two-phase forced convection to the liquid deficient region

Although the transition from two-phased forced convection region to liquid deficient region are not encountered in the experiment, this section is given for the completeness. Lavin & Young's correlation (1956) is used for the determination of transition from two-phase forced convection to the liquid deficient region. Dry-out occurs if the quality exceeds the critical quality defined as

$$h=0.0162\left(\frac{K_g}{D}\right)Re_g^{0.84}Pr_g^{0.33}(1-X_{cr})^{0.1} \tag{18}$$

In this region, Rhee and Young's correlation (1974) for x_{cr} is used.

$$X_{cr}=\left[\frac{We\sigma\rho_g}{W_l\mu_l\left\{\frac{Re_l}{(1-\alpha)^{0.125}}\right\}}\right]^{0.5}, \text{ where}$$

$$We=1.87\times10^{-7}Re_g\left(\frac{\rho_l}{\rho_g}\right)\left(\frac{D}{0.0608}\right)^{-0.48} \tag{19}$$

2.4.4 Dryout region

In this region the heat transfer coefficient decreases as the quality increases and reaches a minimum equal to that of single phase vapor when $x=1$. The effective heat transfer for this region is calculated by Ali and McDonald (1977) as followings;

$$h_{e3}=Ah_v+Bh_{el} \text{ where } A=\frac{(X-X_{cr})}{1-X_{cr}},\quad B=1-A \tag{20}$$

The single-phase vapor heat transfer coefficient was calculated under the assumption that vapor alone occupied in the region between the outlet end of the condenser and the end of the evaporator. The pressure drop in this region decreases as the quality increases. The following method was adopted from literature, where the frictional pressure drop was calculated as a function of x. The relation used in the program to calculate the frictional pressure drop for the dryout region was as following:

$$\Delta P_{f,do}=(C\Delta P_{f,g}+D\Delta P_{f,tp}) \tag{21}$$

where,

$$C=\frac{x-x_{cr}}{1-x_{cr}}, \text{ and } D=1-C \text{ at } x=x_{cr},\ \Delta P_{f,do}=\Delta P_{f,tp} \text{ and at } x=l,\ \Delta P_{f,do}=\Delta P_{f,g} \tag{22}$$

The pressure drop decreases linearly with the increase of x_{cr} between the above two limits. The hydrostatic and acceleration pressure drops were calculated in a manner similar to relations that described in the calculation of the two-phase flow pressure drop.

2.4.5 Single-phase vapor flow

As the flow progresses up, the magnitude of the quality reaches 1.At this region, the flow is in vapor phase and the relations described in section single phase flow are used for the estimation of the heat transfer coefficient for this region using vapor properties instead of the liquid properties. Since the flow is all vapor, the pressure drop ss calculated from the relations as indicated in section single phase flow by using vapor properties.

If the vapor is in a superheated state, vapor desuperheating takes place and the wall temperature is calculated using the single-phase vapor heat transfer correlations. Condensation heat transfer takes place when vapor is cooled sufficiently below the saturation temperature. The equations used in the determination of the condensation coefficient are given in Appendix A.

2.5 Fin efficiency

The method of designing cooling fins of various shapes is based on the same principles as those used for calculating the cooling capacity of rods of constant cross-section. The greater the distance from the base of the fins, the smaller the heat flow, so that for constant cross section, the temperature gradient decreases along the fin length. Theoretically, if the heat transfer coefficient is constant, the fin bounded by a pair of parabolas is the most efficient by Hewitt et al. (1994). In practice, the fin of such shape is too difficult to manufacture, thus it is usual to design fins having trapezoidal sections. The present design consisted of thin rectangular fins attached to the cylindrical base of the tubes because of the difficulty of manufacturing fins with the best shape for heat transfer. The fin efficiency of circular or rectangular fins attached to the TLT involved mathematically Bessel functions, which could usually be represented in tabular and graphical forms.

For analysis and simulation, approximate, but reasonably accurate empirical expressions presented by McQuiston and Tree (Hewitt et al., 1994) were used. They commented that the difference between experimental results and results calculated by their empirical equation was $\pm 3 \sim 4$ %. Fins are also used on the liquid side and even with condensing vapors having low heat transfer coefficients.

$$\eta_f = \frac{\tan h(m\Psi)}{m\Psi} \tag{23}$$

Heat transfer from a prime surface can be increased by attaching fins or extended surfaces. Use of a finned cooling surface is particularly effective in the case where the heat transfer coefficient between the wall and one fluid is substantially greater than the heat transfer coefficient to the other fluid. Thus, fins on pipes are very effective when liquid flows inside the pipe and gas flows on the outside. The fin efficiency was collected and evaluated for its applicability in Appendix B. The conduction shape factor needed for the evaporator section was estimated by analytical solutions from the literature.

3. Simulation Technique

The simulation computer code was developed with the following environments:

a. Program language: Microsoft Visual Basic CCE 5.0

b. Programming environment: Microsoft Windows 95

c. Working environment: Microsoft Windows 95

d. Programming method: The simulation computer code for the cooling system of the present study was developed for general use. The simulation model, which was derived from the ideal model shown in the TLT proposed from the proceeding paper, was based on a sectorial thermal resistance network as shown in Fig. 1.

3.1 Program logic

The model used for the development of a computer simulation program was based on the following assumptions with;

a. one dimensional steady state equilibrium flow,

b. the homogeneous model for two-phase regions,

c. a linear variation of the quality of the vapor in the two-phase zone from one section boundary to the other

d. radiation exchanges with the surroundings are negligible.

The equations used in the model were taken from the open literature. Due to many possible modes of heat transfer that might occur along the loop and within the evaporator section, the loop was analyzed by subdividing the loop into shorter elemental lengths for which average values would

provide a better approximation.

One difficulty encountered in developing the simulation code for systems such as that in the present study was that some of the correlations available had to be used for the conditions beyond the range of variables over which they were established. The second difficulty was the determination of the best method to handle the transition regions between the various flow regimes occurred in the evaporator section. Various parameters such as velocity, void fraction and quality are to be used to determine the transition regions. The third difficulty to be encountered is that the pressure drop must be analyzed to converge the entire simulation result.

The whole simulation procedure is shown in the flow chart of Fig. 2. The program would estimate an initial pressure and temperature in the evaporator liquid inlet port and the mass flow rate of the thermosyphon loop, then proceed to calculate the heat transfer, the exit state of the working fluid and the fluid temperature downstream of the evaporator. The pressure drop across and the heat loss along the section between the evaporator and condenser sections are to be

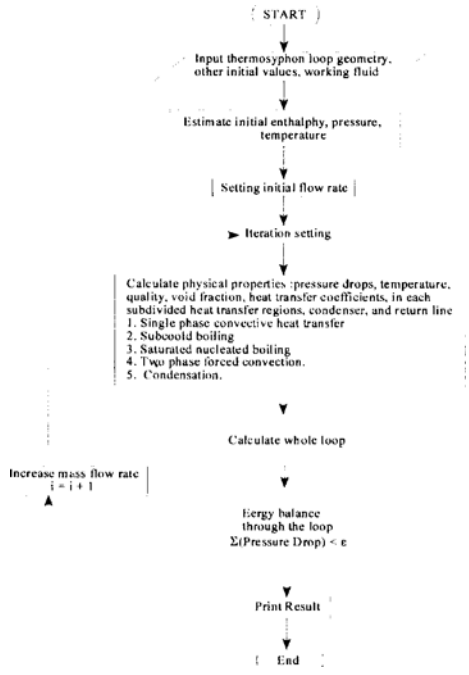

Fig. 2 Algorithm for the proposed TLT system.

calculated. Assuming a negligible pressure drop along the condenser section, and by knowing the inlet and the exit states of the condenser, the heat transfer in condenser and the temperature of the fluid leaving the condenser section are to be calculated. The inlet pressure of the evaporator section is to be varied until the incoming liquid temperature is achieved. Once this convergence is reached, an energy balance applied to the evaporator section would yield a new value for the fluid temperature at the inlet port of the evaporator section. This new value is used to generate the final values including the static liquid level, which would exist in the loop upon shutdown.

3.2 Thermal properties and operating limit

As stated by Rhie, et al. (1997), the thermal properties of the working fluids, which were used in the simulation computer code, such as the density, viscosity and pressure versus saturation temperature, were calculated using the generally accepted method and approximations given in Reid and Sherwood (1996). These calculations were necessary because of the lack of published data, especially for FC-72 and FC-87.Results of calculations involving FC-72 and FC-87 when compared with a few known thermal properties showed about 10 % difference by Rhie, et al. (1997) The thermal properties of other working fluids were formulated into empirical equations using data regression for the temperature range of -50 °C to 150 °C. The analysis of these equations for the thermal properties of each working fluid showed the difference of about ± 5 %.

In the TLT, heat is transported upward by the vapor generated in the heating section. The vapor flows up through the connecting transport tube and condenses in the cooling section. The condensate is then returned to the heating section by gravity. However, when the heat- transport rate is increased greatly, a limiting point may be reached where a sharp rise in wall temperature or sharp deterioration in heat transfer coefficients takes place in the heating section. Many investigators have studied this performance limit and it can be noted that the limit can be classified into two types.

The first type of performance limit occurs at very low liquid fill charges. There is a minimum quantity of working fluid required for the TLT to have a continuous circulation of vapor and condensate in accordance with the heat transport rate. If the quantity of working fluid is less than the required minimum, the returning liquid may not reach the heating section in time, resulting in dry-out of the heating section, or that the wall temperature slowly rises. Thus, this type is usually called the dry-out limit. The second type occurs when the heating surface is covered by vapors. Vapor bubbles are generated in the liquid pool of the evaporator section, and this nucleate boiling becomes more intense with increase of heat flux. At a certain critical radial heat flux, individual vapor bubbles are combined to form rather quickly a vapor film at the wall. This vapor film insulates the evaporator surface from the evaporating liquid. Owing to the poor thermal conductivity of the vapor, only part of the heat input to the wall cause a sudden increase of the evaporator wall temperature. This boiling limit called burn-out limit. This limit may prevail for relatively large liquid fill charges.

Since the present model is charged with a sufficient amount of working fluid and the heat flux is relatively moderate, the first and second types of the operating limits are not considered.

3.3 Simulation

Based on the above assumptions, the code was simulated with following parameters; all necessary dimensions of a TLT such as the diameter, lengths, and material thermal conductivities. Correlations for heat transfer coefficients of evaporation, condensation, and forced convection can be specified. In a two dimensional system which only two temperature limits are involved, it is possible to define conduction shape factor S. In reality, the effect of S can be negligible, but in the simulation code all possible parameters are considered. Shape factors for a rectangular pipe in a semi-infinite solid medium is installed in the simulation code. The present simulation model has rectangular fins with an annular base. In the simulation code, two kinds of fin are provided: rectangular fins and circular fins with an annular base. As stated previously, a mathematical solution of fin efficiency involves Bessel functions, but in the present simulation code, the complex exact solution would reduce the speed of computation. This empirical correlation has a $\pm 3 \sim 4$ % error. Based on all these described parameters, the calculation would be proceeding.

The process presents the simulation progress, and the results, such as the cooling rate, saturation temperature, and pressure. Once this convergence is reached, energy, momentum, mass balances applied to the system would yield a new value for the fluid temperature at the inlet port of the evaporator section. This routine leads to generate the next iteration. In momentum balance, the summation of the pressure drop through the loop system is set to ε.

$$\sum(\textit{Residual of Pressure drop}) < \varepsilon$$

In simulation, the convergence criteria, ε is defined as the accuracy ranging from 10^{-1} to 10^{-5}. Obviously, increasing the precision of ε determined by selection from the program window will lengthen the computational time to derive the nodal values. The processing allows many trials with different working fluids to contrast their heat transfer capabilities. No attempt was made to include the operational limits because dry-out and burn-out as which were not yet well documented. From repetitive trials with a change of specific parameters for the shape factor, fin specification, some correlation sources, and correction factor, the simulated temperature profile were obtained.

4. Results and Discussions

The ultimate test of a computer simulation code is to compare the simulation results with the experimental data. Only when the code is verified, its usefulness is authenticated. Since the present simulation is for the two-phase flow and heat transfer in a small loop type two-phase thermosyphon which involves a large number of empirical correlations, one must be careful to run the code not only for the final results (macroscopic) but

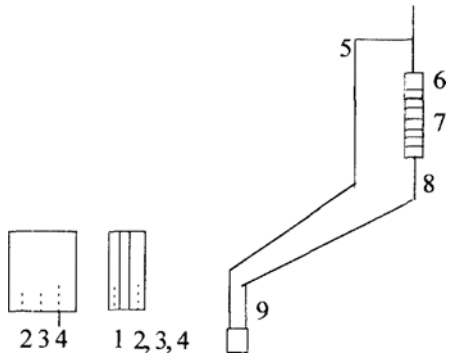

Fig. 3 Thermocople identification in the schematic of TLT.

for the crucial elements which would determine the final outcome.

It was shown by Rhie, et al. (1997) that the success of the computer code for a TCT strongly depended on the choice of empirical correlations required for various thermal resistances used in the analysis. The crucial element is the temperature distribution along the loop of the TLT. It is clearly seen that a computer code alone can not give any meaningful quantitative results unless it is accompanied by some experimental results, meaning that no computer code should be developed without a benchmark experimental verification. Figure 3 identifies the location of thermocouples of the proposed TLT system in the experimental result.

Figures 4(a) to (c) show the comparison of the experimental results on heat transfer rate of the system as a function of the interior simulated temperature difference between the evaporator and the ambient air. In spite of difficulties involved in choosing the right combination for the empirical equations used in the simulation through the TLT system proposed in the experimental result, the agreement is very good. From the assumption for an initial value for Ti for each location located from Fig. 2, heat load, Q, obtained as a final result might have a little difference between the simulation and experiment results. The simulation predicts correctly not only the effect of the working fluid but also the magnitude of the heat transfer rate. Under the natural convection mode of the TLT with FC-87 as the

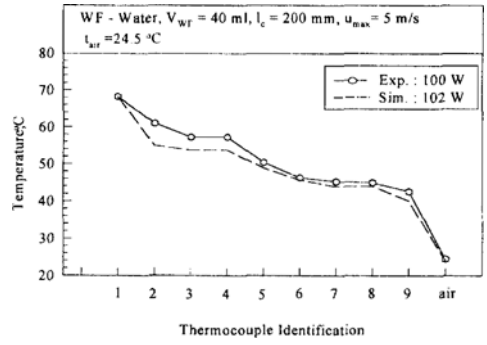

(a) WF=water

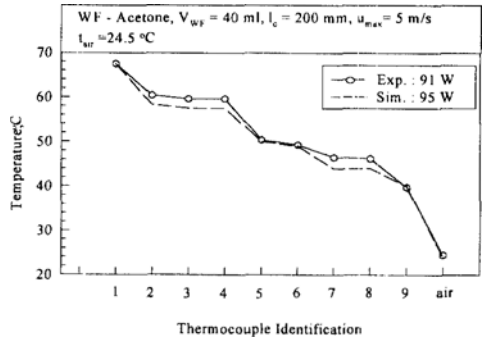

(b) WF=acetone

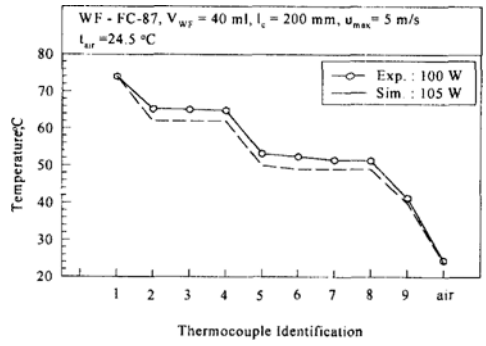

(c) WF=FC-87

Fig. 4 Temperature distribution between simulation and experiment.

working fluid as shown in Fig. 4(c), the cooling capacity is achieved up to heat transfer rate of 105 W, where heat flux is approximately up to 8.6 W/cm^2, with the overall temperature difference of 50℃.

Since the solution required for the code is based on the sectorial thermal resistance which require a large number of empirical correlations, the key to check the correctness of the code is to

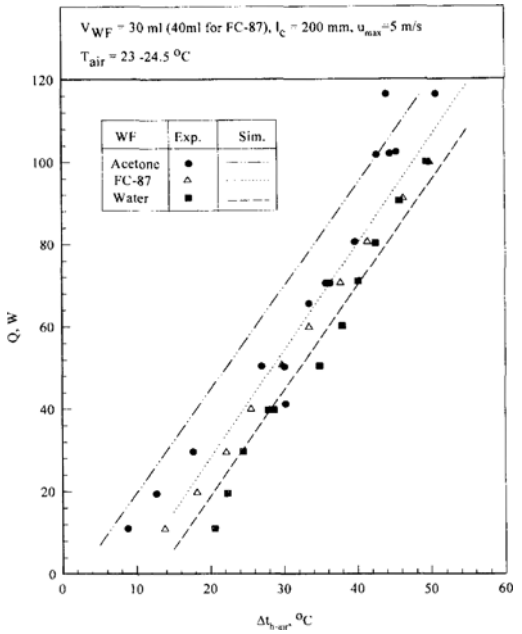

Fig. 5 Comparison of simulation with experiments of the proceeding paper.

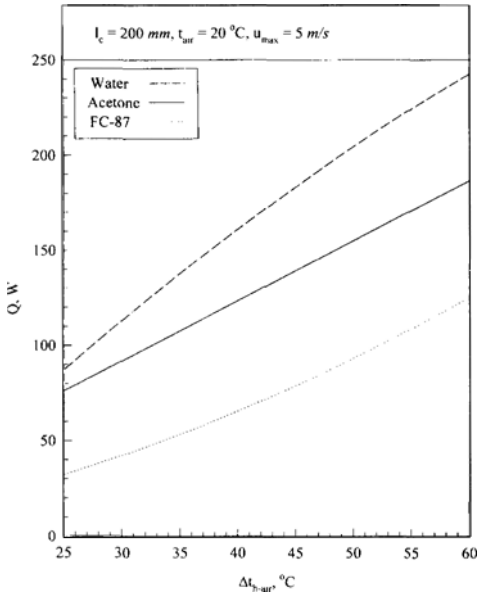

Fig. 6 Effect of Δt_{h-air} on heat transfer rate.

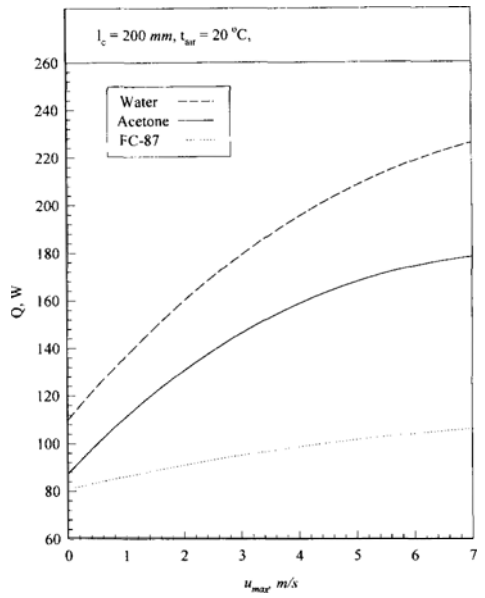

Fig. 7 Effect of $u_{\max}$ on Q.

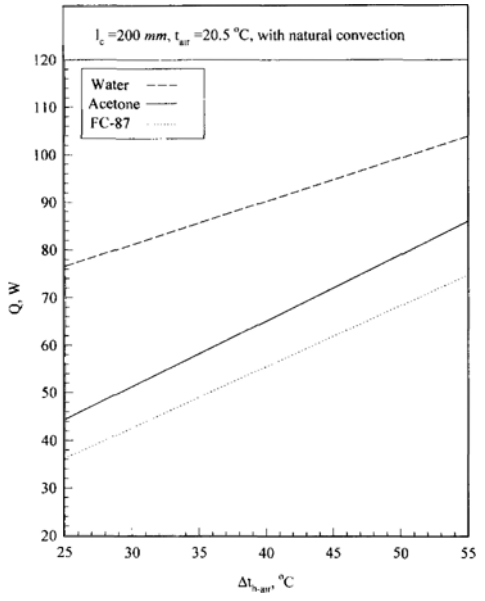

Fig. 8 Effect of Δt_{h-air} on Q.

compare the temperature distribution within the TLT obtained by the simulation with that of the experiments. With these empirical correlations as shown in Appendix, it is now possible to compare the simulation results with the experimental results for the effects of the various parameters. The simulation results for the effect of three working fluids on heat transfer rate, Q (W), with respect to the temperature difference between heater and air, Δt_{h-air}, under the forced convection were illustrated in Fig. 5. The simulated temperature distribution along the TLT could be

slightly different from the experimental results, depending on the choice of the empirical equations used for various modes of the heat transfer involved, although the final heat transfer rates might reasonably agree each other.

Figures 6 and 7 show the heat transfer rate, Q (W), for the effects of the saturation temperature of the working fluid and the air velocity on the condenser section, u_{max} (m/s), in the TLT with forced convection mode. As seen in Fig. 6, in the loop thermosyphon system, cooling heat flux is capable of carrying a little over 15 W/cm^2 with the overall temperature difference of 50°C under the forced convection when water is used as the working fluid.

And the effect of three working fluids on Q vs. t_{h-air} under the natural convection is illustrated in Fig. 8.

5. Concluding Remarks

For the two-phase loop thermosyphon system proposed in the proceeding paper, the simulation code based on the sectorial thermal resistance is built and the following conclusions are made:

(1) From the corrected empirical correlations accompanied with some benchmark elements used in the simulation, the effect of the working fluid as well as the magnitude of the heat transfer rate was predicted and the agreement with the experimental results was very good.

(2) The aim of the cooling capacity up to a heat flux of 15 W/cm^2 was achieved under the forced convection mode cooling.

(3) Under the natural convection mode with FC-87 as the working fluid, the cooling capacity was achieved up to heat flux of 8.6 W/cm^2.

(4) The heat transfer rate was found to be increased gradually with saturation temperature.

References

Ali A. F. M. and McDonald, T. W. 1977, "Thermosyphon Loop Performance Characteristics: Part 2, Simulation Program," *ASHRAE trans.*, Vol. 83, pt. 2, pp. 260~278.

Bejan, A. 1993, *Heat Transfer*, John, Wiley & Sons Inc., New York.

Collier, J. G. 1972, *Convective Boiling and Condensation, 2nd edition*, McGraw-Hill Book Company, New York.

Faghri, A. 1995, *Heat Pipe Science and Technology*, Taylor & Francis, Washington, DC.

Hewitt, G. F. Shiress and G. L. Bott, T. R. 1994, *Process Heat Transfer*, CRC Press, London.

Holman, J. P. 1996, *Heat Transfer*, 8th ed., McGraw-Hill, New York.

Ito, H. 1960, "Pressure Losses in Smooth Pipe Bends," *ASME Trans., Ser. D, Journal of Basic Engineering*, vol. 82 (1), No. 13.

Kutateladze, S. S. 1963, *Fundamentals of Heat Transfer*, Edward Arnold Ltd., New York.

Kishimoto, T. et al., 1994, "Heat Pipe Cooling Technologies for Telecom JMCM's," *Proceedings of 4th Int. Heat Pipe Symposium*, Tsukuba, pp. 132~141.

Lavin and J. G. Young, H. Y. 1956, "Heat Transfer to Evaporating Refrigerants in Two-Phase Flow," *A. I. Ch. E. J*, Vol. 11, No. 6, p. 1124.

Mathur, C. D. 1996, *A Simulation Program for Multiple Tube-Row Two-Phase Thermosyphon Coil Loop Heat Exchangers*, Ph. D Thesis, University of Windsor.

Reid R. C. and Sherwood, T. K. 1966, *The Properties of Gases and Liquids*, 2th ed., McGraw-Hill, New York.

Rhee B. W. and Young, H. Y. 1974, "Heat Transfer to Boiling Refrigerants Flowing Inside a Plaing Copper Tube," *A. I. Ch. E. Symposium, Series* 64.

Rhi, S. H. Kim, W. T. and Lee, Y. 1997, "A Cooling System Using Wickless Heat Pipes for Multichip Modules: Experiment and Analysis" *KSME Int. J.*, Vol. 11 No. 2, pp. 208~220.

Sato T. and Matsumura, H. 1964, "On the Conditions of Incipient Subcooled Boiling and Forced Convection," *JSME*, Vol. 7, No. 36, pp. 392~398.

Sieder and E. N. Tate, G. E. 1936, "Heat Transfer and Pressure Drop of Liquids in Tubes," *Industrial and Eng., Chemistry*, Vol. 28, No. 12, pp. 1429.

Appendix

A. Correlations for heat transfer coefficient

Boiling	Dengler-Adams (1956) (Mathur, 1996) A and n are constants.	$\frac{h_{tp}}{h_{lp}}=A\left(\frac{1}{X_{tt}}\right)^n$ $h_{tp}=0.023\frac{K_{ll}}{D}\left[\frac{DW_T(1-x)}{\mu_{tp}}\right]Pr_l^{0.4}$ $\frac{1}{X_{tt}}=\left(\frac{x}{1-x}\right)^{0.9}\left(\frac{\rho_l}{\rho_v}\right)^{0.5}\left(\frac{\mu_v}{\mu_l}\right)^{0.4}$
	Davis and David (1961) (Mathur, 1996)	$h_{tp}=0.0333\frac{K_l}{D}\left[\frac{DW_T}{\mu_{tp}}\right]Pr_l^{0.4}$; $\frac{1}{\mu_{tp}}=\frac{x}{\mu_T}+\frac{1-x}{\mu_l}$
Condensation	Nusselt (1916) (Ali and Mcdonald, 1977)	$h_c=0.943\left[\frac{k_l\rho_l(\rho_l-\rho_g)\,gh_{fg}}{\mu_l\Delta t_{sat}L_c}\right]$
	Rohsenow (1956) (Holman, 1996)	$h_c=0.943\frac{k_l}{L_c}\left[\frac{l_c^3\rho_l(\rho_l-\rho_g)\,g}{\mu_l\Delta t_{sat}k_l}[h_{fg}+0.68c_{pl}\Delta t_{sat}]\right]^{1/4}$
	Ali and McDonald (1977) (Holman, 1996)	$h_c=B_1\left[\frac{k_l^3\rho_l^2gh_{fg}}{\mu_lD\Delta t_{sat}}\right]^{1/4}$ for $0°<\beta<40°$; $B_1=0.727$ for $40°<b<90°$; $B_1=0.727\left[\cos\left(\frac{\beta-40}{50}\right)90\right]^{1/4}$
Forced convection from a finned area	Knudsen and Katz (1958) (Holman, 1996)	$\frac{hd}{k_f}=C\left[\frac{u_\infty D}{\gamma_f}\right]^nPr^{1/3}$ $C=0.683$, $n=0.466$ for $40<Re<4000$
	Fand (1965) (Holman, 1996)	$Nu_f=(0.35+0.65Re_f^{0.52})\,Pr_f^{0.3}$
	Churchill and Bernstein (1977) (Holman, 1996)	$Nu=0.3+\frac{0.62Re^{1/2}Pr^{1/3}}{\left[1+(0.4/Pr)^{2/3}\right]}\left[1+\left(\frac{Re}{282000}\right)^{5/8}\right]^{4/5}$
Natural convection	Without air flow in the condenser section (Bejan, 1993)	$Nu=\frac{4}{3}\left[\frac{7Ra\mathrm{Pr}}{5(20-21\mathrm{Pr})}\right]^{1/4}+\frac{4(272+315\mathrm{Pr})\,L_c}{35(64+63\mathrm{Pr})\,D}$

B. Fin efficiency

The total fin efficiency (Hewitt, et al., 1994)	$\eta_T=1-\frac{A_{fin}}{A_T}(1-\eta_{fin})$, $A_T=A_{fin}+A_t$, $A_T=\pi d(L_c-N_{fin}\delta_{fin})$ $\eta_{fin}=\frac{\tan h(m\Psi)}{m\Psi}$, $m=\sqrt{\frac{2h_{conv}}{k_{fin}\delta_{fin}}}$, $h_{conv}=\frac{Nuk}{D}$ $\Psi=\frac{D_i}{2}\left[\left(\frac{r_e}{r_i}\right)-1\right]\left[1+0.35\ln\left(\frac{r_e}{r_i}\right)\right]$	
	for annular fins	$\frac{r_e}{r_i}=\frac{r_o}{r_i}$
	for rectangular fins	$\frac{r_e}{r_i}=1.28\frac{L_{horizontal}}{L_{vertival}}\sqrt{\frac{L_{horizontal}}{L_{vertival}}-0.2}$

C. Pressure drop calculations in single-phase

Frictional pressure drop	straight pipe (Collier, 1972)	$\Delta P_f = 4f\frac{\Delta y v_l^2}{2D}\rho_l$ for laminar flow (Re<2000), $f=16/\mathrm{Re}$ for turbulent flow (Re>2000), $f=0.079/\mathrm{Re}^{0.25}$
	Bended pipe (Ito, 1960):	$\Delta P_f = 0.0024 a_b \partial \left(\frac{G_b D_b}{\mu_l}\right)^{-0.17}\left(\frac{2R}{D_h}\right)^{0.84}\left(\frac{G_b^2}{\rho_l}\right)$ $a_b=1$ for $2R/D_b>19.7$ $a_b=0.95+17.2(2R/D_b)^{-1.96}$ for $2R/D_b<19.7$
	Entrance (Collier, 1972)	$\Delta P_f = (1+\zeta)\left(\frac{G_b^2}{2\rho_l}\right)$
	Area expansion (Collier, 1972):	$\Delta P_f = \frac{G_l^2}{2}(1-\alpha^2)\nu_l\left(1+\frac{\nu_g}{\nu_l}\right)$
	Area contraction (Collier, 1972):	$\Delta P_f = \left[\left(\frac{1}{C_c}-1\right)^2+1-\left(\frac{A}{A_b}\right)^2\right]\left(\frac{G^2}{2\rho_l}\right)$
Hydrostatic pressure drop	Collier, 1972	$\Delta P_{tph} = \Delta y\, \rho g \sin\gamma$
Acceleration pressure drop	Lockhart and Martinelli, 1949 (Collier, 1972)	$\Delta P_a = \frac{G_l^2}{\rho_l}\left[\frac{(1-x)^2}{1-\alpha}+\left(\frac{x^2}{\alpha}\right)\left(\frac{\rho_l}{\rho_v}\right)-1\right]$